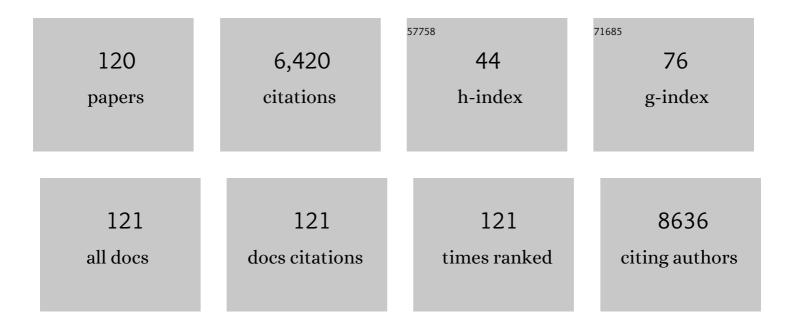
List of Publications by Year in descending order

Source: https://exaly.com/author-pdf/9222505/publications.pdf Version: 2024-02-01



#	Article	lF	CITATIONS
1	Hierarchically porous carbon by activation of shiitake mushroom for capacitive energy storage. Carbon, 2015, 93, 315-324.	10.3	395
2	Biomass-Derived Carbon Fiber Aerogel as a Binder-Free Electrode for High-Rate Supercapacitors. Journal of Physical Chemistry C, 2016, 120, 2079-2086.	3.1	274
3	Swelling and Delamination Behaviors of Birnessite-Type Manganese Oxide by Intercalation of Tetraalkylammonium Ions. Langmuir, 2000, 16, 4154-4164.	3.5	234
4	Three-Dimensional Tubular MoS ₂ /PANI Hybrid Electrode for High Rate Performance Supercapacitor. ACS Applied Materials & Interfaces, 2015, 7, 28294-28302.	8.0	231
5	Activation of graphene aerogel with phosphoric acid for enhanced electrocapacitive performance. Carbon, 2015, 92, 1-10.	10.3	193
6	A high-energy-density supercapacitor with graphene–CMK-5 as the electrode and ionic liquid as the electrolyte. Journal of Materials Chemistry A, 2013, 1, 2313.	10.3	186
7	Telluriumâ€Assisted Epitaxial Growth of Largeâ€Area, Highly Crystalline ReS ₂ Atomic Layers on Mica Substrate. Advanced Materials, 2016, 28, 5019-5024.	21.0	169
8	Graphene–MnO2 and graphene asymmetrical electrochemical capacitor with a high energy density in aqueous electrolyte. Journal of Power Sources, 2011, 196, 10782-10787.	7.8	161
9	Phase Transition Behavior and Large Piezoelectricity Near the Morphotropic Phase Boundary of Leadâ€Free (<scp><scp>Ba</scp></scp> _{0.85} <scp><scp>Ca</scp></scp> _{0.15})(<scp><scp>ZrCeramics, Journal of the American Ceramic Society, 2013, 96, 496-502.</scp></scp>	:p> ^{3;8} scp>	_{0.1}
10	Thin‧heet Carbon Nanomesh with an Excellent Electrocapacitive Performance. Advanced Functional Materials, 2015, 25, 5420-5427.	14.9	139
11	Creation of nanopores on graphene planes with MgO template for preparing high-performance supercapacitor electrodes. Nanoscale, 2014, 6, 6577-6584.	5.6	127
12	RuO2/graphene hybrid material for high performance electrochemical capacitor. Journal of Power Sources, 2014, 248, 407-415.	7.8	120
13	Layer-Stacking Activated Carbon Derived from Sunflower Stalk as Electrode Materials for High-Performance Supercapacitors. ACS Sustainable Chemistry and Engineering, 2018, 6, 11397-11407.	6.7	118
14	Morphological and Interfacial Control of Platinum Nanostructures for Electrocatalytic Oxygen Reduction. ACS Catalysis, 2016, 6, 5260-5267.	11.2	117
15	Giant Dielectric Constant and Good Temperature Stability in <scp><scp>Y</scp></scp> _{2/3} <scp><cp>Cu</cp></scp> ₃ <scp><scp>TiCeramics. Journal of the American Ceramic Society, 2012, 95, 2218-2225.</scp></scp>	>< 318 b>4<	/suba <scp></scp>
16	Highly Compressible Carbon Sponge Supercapacitor Electrode with Enhanced Performance by Growing Nickel–Cobalt Sulfide Nanosheets. ACS Applied Materials & Interfaces, 2018, 10, 10087-10095.	8.0	111
17	Graphene/VO2 hybrid material for high performance electrochemical capacitor. Electrochimica Acta, 2013, 112, 448-457.	5.2	107
18	Synthesis of Large‣ize 1T′ ReS ₂ <i>_x</i> Se _{2(1â^'} <i>_x</i> Alloy Monolayer with Tunable Bandgap and Carrier Type. Advanced Materials, 2017, 29, 1705015.	21.0	107

#	Article	IF	CITATIONS
19	δ-MnO ₂ /holey graphene hybrid fiber for all-solid-state supercapacitor. Journal of Materials Chemistry A, 2016, 4, 9088-9096.	10.3	101
20	Holey nickel-cobalt layered double hydroxide thin sheets with ultrahigh areal capacitance. Journal of Power Sources, 2018, 387, 108-116.	7.8	97
21	Formation process of holey graphene and its assembled binder-free film electrode with high volumetric capacitance. Electrochimica Acta, 2016, 187, 543-551.	5.2	94
22	Facile Electrochemical Fabrication of Porous Fe ₂ O ₃ Nanosheets for Flexible Asymmetric Supercapacitors. Journal of Physical Chemistry C, 2017, 121, 18982-18991.	3.1	90
23	Holey graphene/polypyrrole nanoparticle hybrid aerogels with three-dimensional hierarchical porous structure for high performance supercapacitor. Journal of Power Sources, 2016, 317, 10-18.	7.8	87
24	CoNi ₂ S ₄ Nanoparticle/Carbon Nanotube Sponge Cathode with Ultrahigh Capacitance for Highly Compressible Asymmetric Supercapacitor. Small, 2018, 14, e1800998.	10.0	87
25	Preparation and capacitive property of manganese oxide nanobelt bundles with birnessite-type structure. Journal of Power Sources, 2011, 196, 855-859.	7.8	86
26	Preparation of Ag-Nanoparticle-Loaded MnO ₂ Nanosheets and Their Capacitance Behavior. Energy & Fuels, 2012, 26, 618-623.	5.1	82
27	Design of Palladium-Doped <i>g</i> -C ₃ N ₄ for Enhanced Photocatalytic Activity toward Hydrogen Evolution Reaction. ACS Applied Energy Materials, 2018, 1, 2866-2873.	5.1	76
28	Effects of Li content on the phase structure and electrical properties of lead-free (K0.46â^'xâ^•2Na0.54â^'xâ^•2Lix)(Nb0.76Ta0.20Sb0.04)O3 ceramics. Applied Physics Letters, 2007, 90, 232905.	3.3	73
29	Phase transitional behavior, microstructure, and electrical properties in Ta-modified [(K0.458Na0.542)0.96Li0.04]â€^NbO3 lead-free piezoelectric ceramics. Journal of Applied Physics, 2008, 104, .	2.5	72
30	Reduced graphene oxide/Mn 3 O 4 nanocrystals hybrid fiber for flexible all-solid-state supercapacitor with excellent volumetric energy density. Electrochimica Acta, 2017, 242, 10-18.	5.2	71
31	High-energy asymmetric electrochemical capacitors based on oxides functionalized hollow carbon fibers electrodes. Nano Energy, 2016, 30, 9-17.	16.0	70
32	Direct growth of flake-like metal-organic framework on textile carbon cloth as high-performance supercapacitor electrode. Journal of Power Sources, 2019, 428, 124-130.	7.8	70
33	Epitaxial growth of large-area and highly crystalline anisotropic ReSe2 atomic layer. Nano Research, 2017, 10, 2732-2742.	10.4	69
34	Nitrogen-doped carbon sheets coated on CoNiO ₂ @textile carbon as bifunctional electrodes for asymmetric supercapacitors. Journal of Materials Chemistry A, 2019, 7, 4165-4174.	10.3	67
35	Fullâ€Temperature Allâ€Solidâ€State Ti ₃ C ₂ T <i>_x</i> /Aramid Fiber Supercapacitor with Optimal Balance of Capacitive Performance and Flexibility. Advanced Functional Materials, 2021, 31, 2010944.	14.9	63
36	Coral-like PEDOT Nanotube Arrays on Carbon Fibers as High-Rate Flexible Supercapacitor Electrodes. ACS Applied Energy Materials, 2020, 3, 7794-7803.	5.1	55

#	Article	IF	CITATIONS
37	Ti ₃ C ₂ T _{<i>x</i>} Nanosheets/Ti ₃ C ₂ T _{<i>x</i>} Quantum Dots/RGO (Reduced) Tj ETQq1 1 C	0.784314 r 8.0	gBT/Overloc
38	Density and Good Flexibility. ACS Applied Materials & amp: Interfaces, 2020, 12, 11833-11842. Ultraâ€Large Sized Siloxene Nanosheets as Bifunctional Photocatalyst for a Liâ€O ₂ Battery with Superior Roundâ€Trip Efficiency and Extraâ€Long Durability. Angewandte Chemie - International Edition, 2021, 60, 11257-11261.	13.8	53
39	Textile carbon network with enhanced areal capacitance prepared by chemical activation of cotton cloth. Journal of Colloid and Interface Science, 2019, 553, 705-712.	9.4	51
40	Enhancing the Capacitive Performance of Carbonized Wood by Growing FeOOH Nanosheets and Poly(3,4-ethylenedioxythiophene) Coating. ACS Applied Materials & Interfaces, 2018, 10, 32192-32200.	8.0	50
41	Functional graphene nanocomposite as an electrode for the capacitive removal of FeCl3 from water. Journal of Materials Chemistry, 2012, 22, 14101.	6.7	48
42	Metallic-Phase MoS ₂ Nanopetals with Enhanced Electrocatalytic Activity for Hydrogen Evolution. ACS Sustainable Chemistry and Engineering, 2018, 6, 13435-13442.	6.7	48
43	Free-standing graphene/bismuth vanadate monolith composite as a binder-free electrode for symmetrical supercapacitors. RSC Advances, 2018, 8, 24796-24804.	3.6	48
44	Intercalation and delamination behavior of Ti ₃ C ₂ T _x and MnO ₂ /Ti ₃ C ₂ T _x /RGO flexible fibers with high volumetric capacitance. Journal of Materials Chemistry A, 2019, 7, 12582-12592.	10.3	48
45	Capacitive performance of porous carbon nanosheets derived from biomass cornstalk. RSC Advances, 2017, 7, 1067-1074.	3.6	44
46	Î-MnO ₂ nanofiber/single-walled carbon nanotube hybrid film for all-solid-state flexible supercapacitors with high performance. Journal of Materials Chemistry A, 2017, 5, 19107-19115.	10.3	44
47	Enhanced high-order ultraviolet upconversion luminescence in sub-20 nm β-NaYbF ₄ :0.5% Tm nanoparticles via Fe ³⁺ doping. CrystEngComm, 2017, 19, 1304-1310.	2.6	43
48	Facile synthesis of Ti ₄ O ₇ on hollow carbon spheres with enhanced polysulfide binding for high-performance lithium–sulfur batteries. Journal of Materials Chemistry A, 2019, 7, 10494-10504.	10.3	43
49	Phase coexistence and high electrical properties in (KxNa0.96â^'xLi0.04)(Nb0.85Ta0.15)O3 piezoelectric ceramics. Journal of Applied Physics, 2009, 105, 054101.	2.5	41
50	A new type of ordered mesoporous carbon/polyaniline composites prepared by a two-step nanocasting method for high performance supercapacitor applications. Journal of Materials Chemistry A, 2014, 2, 16715-16722.	10.3	40
51	Hierarchical graphene network sandwiched by a thin carbon layer for capacitive energy storage. Carbon, 2017, 113, 100-107.	10.3	39
52	Battery-type graphene/BiOBr composite for high-performance asymmetrical supercapacitor. Journal of Alloys and Compounds, 2020, 812, 152087.	5.5	39
53	Sub-10 nm Water-Dispersible β-NaGdF ₄ : <i>X</i> % Eu ³⁺ Nanoparticles with Enhanced Biocompatibility for in Vivo X-ray Luminescence Computed Tomography. ACS Applied Materials & Interfaces, 2017, 9, 39985-39993.	8.0	38
54	All solid-state V2O5-based flexible hybrid fiber supercapacitors. Journal of Power Sources, 2017, 371, 18-25.	7.8	36

#	Article	IF	CITATIONS
55	Connecting PEDOT Nanotube Arrays by Polyaniline Coating toward a Flexible and High-Rate Supercapacitor. ACS Sustainable Chemistry and Engineering, 2021, 9, 4146-4156.	6.7	36
56	Phase Structure, Microstructure, and Electrical Properties of Sbâ€Modified (K, Na, Li) (Nb, Ta) O ₃ Piezoelectric Ceramics. Journal of the American Ceramic Society, 2008, 91, 2211-2216.	3.8	33
57	Mn 3 O 4 nanocrystalline/graphene hybrid electrode with high capacitance. Electrochimica Acta, 2016, 188, 398-405.	5.2	33
58	Hollow Structure VS ₂ @Reduced Graphene Oxide (RGO) Architecture for Enhanced Sodiumâ€ion Battery Performance. ChemElectroChem, 2020, 7, 78-85.	3.4	33
59	Ethanol-tolerant polyethyleneimine functionalized palladium nanowires in alkaline media: the "molecular window gauze―induced the selectivity for the oxygen reduction reaction. Journal of Materials Chemistry A, 2015, 3, 21083-21089.	10.3	32
60	Simultaneous enhancement of red upconversion luminescence and CT contrast of NaGdF ₄ :Yb,Er nanoparticles <i>via</i> Lu ³⁺ doping. Nanoscale, 2018, 10, 20279-20288.	5.6	32
61	Few-layer and large flake size borophene: preparation with solvothermal-assisted liquid phase exfoliation. RSC Advances, 2020, 10, 27532-27537.	3.6	32
62	Solvothermal-assisted liquid-phase exfoliation of large size and high quality black phosphorus. Journal of Materiomics, 2018, 4, 129-134.	5.7	31
63	MnO ₂ nanoflakes grown on 3D graphite network for enhanced electrocapacitive performance. RSC Advances, 2014, 4, 30233-30240.	3.6	30
64	Nb ₂ O ₅ Nanoparticles Anchored on an N-Doped Graphene Hybrid Anode for a Sodium-Ion Capacitor with High Energy Density. ACS Omega, 2018, 3, 15943-15951.	3.5	30
65	A one-pot gold seed-assisted synthesis of gold/platinum wire nanoassemblies and their enhanced electrocatalytic activity for the oxidation of oxalic acid. Nanoscale, 2016, 8, 2875-2880.	5.6	29
66	Electrospun Nb2O5 nanorods/microporous multichannel carbon nanofiber film anode for Na+ ion capacitors with good performance. Journal of Colloid and Interface Science, 2020, 573, 1-10.	9.4	29
67	High performance graphene/manganese oxide hybrid electrode with flexible holey structure. Electrochimica Acta, 2014, 129, 237-244.	5.2	28
68	Formation mechanisms of interfaces between different Ti _n O _{2nâ^'1} phases prepared by carbothermal reduction reaction. CrystEngComm, 2019, 21, 524-534.	2.6	28
69	Synthesis and capacitive property of δ-MnO2 with large surface area. Journal of Materials Science, 2012, 47, 999-1003.	3.7	25
70	Sandwich-structured Au@polyallylamine@Pd nanostructures: tuning the electronic properties of the Pd shell for electrocatalysis. Journal of Materials Chemistry A, 2016, 4, 12020-12024.	10.3	25
71	Highly flexible all-solid-state cable-type supercapacitors based on Cu/reduced graphene oxide/manganese dioxide fibers. RSC Advances, 2017, 7, 10092-10099.	3.6	25
72	A Lowâ€Cost and Facile Method for the Preparation of Feâ€N/Câ€Based Hybrids with Superior Catalytic Performance toward Oxygen Reduction Reaction. Advanced Materials Interfaces, 2019, 6, 1900273.	3.7	25

#	Article	IF	CITATIONS
73	MoS ₂ nanosheets grown on hollow carbon spheres as a strong polysulfide anchor for high performance lithium sulfur batteries. Nanoscale, 2020, 12, 23636-23644.	5.6	25
74	Polyaniline Nanorods Grown on Hollow Carbon Fibers as Highâ€Performance Supercapacitor Electrodes. ChemElectroChem, 2016, 3, 1142-1149.	3.4	24
75	Preparation and formation process of $\hat{I}\pm$ -MnS@MoS2 microcubes with hierarchical core/shell structure. Journal of Colloid and Interface Science, 2017, 507, 18-26.	9.4	24
76	Controllable synthesis, characterization, and electrochemical properties of manganese oxide nanoarchitectures. Journal of Materials Research, 2008, 23, 780-789.	2.6	22
77	Thermodynamics and Kinetics Synergetic Phase-Engineering of Chemical Vapor Deposition Grown Single Crystal MoTe ₂ Nanosheets. Crystal Growth and Design, 2018, 18, 2844-2850.	3.0	22
78	A Queueâ€Ordered Layered Mnâ€Based Oxides with Al Substitution as Highâ€Rate and Highâ€Stabilized Cathode for Sodiumâ€Ion Batteries. Small, 2021, 17, e2006259.	² 10.0	22
79	Porous PEDOT Network Coated on MoS ₂ Nanobelts toward Improving Capacitive Performance. ACS Sustainable Chemistry and Engineering, 2020, 8, 12696-12705.	6.7	21
80	3D Hierarchical NiCo ₂ S ₄ Nanoparticles/Carbon Nanotube Sponge Cathode for Highly Compressible Asymmetric Supercapacitors. Energy & Fuels, 2021, 35, 3449-3458.	5.1	21
81	Synthesis of Titanium Molybdenum Nitride-Decorated Electrospun Carbon Nanofiber Membranes as Interlayers to Suppress Polysulfide Shuttling in Lithium–Sulfur Batteries. ACS Sustainable Chemistry and Engineering, 2022, 10, 776-788.	6.7	21
82	Filling Ti3C2Tx nanosheets into melamine foam towards a highly compressible all-in-one supercapacitor. Nano Research, 2022, 15, 3254-3263.	10.4	20
83	Vapor-phase polymerization of fibrous PEDOT on carbon fibers film for fast pseudocapacitive energy storage. Applied Surface Science, 2022, 597, 153684.	6.1	20
84	Rational design and controllable preparation of holey MnO ₂ nanosheets. Chemical Communications, 2017, 53, 2950-2953.	4.1	18
85	(TiO ₂ (B) Nanosheet)/(Metallic Phase MoS ₂) Hybrid Nanostructures: An Efficient Catalyst for Photocatalytic Hydrogen Evolution. Solar Rrl, 2019, 3, 1900323.	5.8	18
86	Hollow Structure VS 2 @Reduced Graphene Oxide (RGO) Architecture for Enhanced Sodiumâ€lon Battery Performance. ChemElectroChem, 2020, 7, 5-5.	3.4	18
87	Controlled synthesis and characterization of layered manganese oxide nanostructures with different morphologies. Journal of Nanoparticle Research, 2009, 11, 1107-1115.	1.9	17
88	Incorporation of electroactive NiCo2S4 and Fe2O3 into graphene aerogel for high-energy asymmetric supercapacitor. Colloids and Surfaces A: Physicochemical and Engineering Aspects, 2020, 602, 125110.	4.7	17
89	Fluoride anions-assisted hydrothermal preparation and growth process of β-MnO2 with bipyramid prism morphology. CrystEngComm, 2013, 15, 6682.	2.6	16
90	Ti3C2Tx/RGO//PANI/RGO all-solid-state asymmetrical fiber supercapacitor with high energy density and superior flexibility. Journal of Alloys and Compounds, 2021, 861, 157950.	5.5	15

#	Article	IF	CITATIONS
91	Novel synthesis and formation process of uniform Mn2O3 cubes. CrystEngComm, 2012, 14, 8253.	2.6	14
92	Mesoporous-assembled MnO ₂ with large specific surface area. Journal of Materials Chemistry A, 2015, 3, 14567-14572.	10.3	14
93	Tuning the catalytic activity of colloidal noble metal nanocrystals by using differently charged surfactants. Nanoscale, 2018, 10, 5607-5616.	5.6	14
94	High-quality borophene quantum dot realization and their application in a photovoltaic device. Journal of Materials Chemistry A, 2021, 9, 24036-24043.	10.3	14
95	Ti2Nb2O9/graphene hybrid anode with superior rate capability for high-energy-density sodium-ion capacitors. Journal of Alloys and Compounds, 2021, 860, 158431.	5.5	14
96	Lithium Storage in Carbon Cloth–Supported KNb 3 O 8 Nanorods Toward a Highâ€Performance Lithiumâ€Ion Capacitor. Small Structures, 2021, 2, 2100029.	12.0	14
97	Boosting Pseudocapacitive Performance of KNb3O8 Nanorods by Growing on Textile Carbon Cloth and Carbon Layer Coating. Journal of Physical Chemistry C, 2020, 124, 11358-11367.	3.1	12
98	Ti3C2Tx/aramid film electrode with high capacitance and good mechanical strength and the assembled wide temperature all-solid-state symmetrical supercapacitor. Journal of Power Sources, 2022, 520, 230899.	7.8	12
99	Synthesis of Ti4O7/Ti3O5 Dual-Phase Nanofibers with Coherent Interface for Oxygen Reduction Reaction Electrocatalysts. Materials, 2020, 13, 3142.	2.9	11
100	Formation Mechanism of Nitrogen-Doped Titanium Monoxide Nanospheres and Their Application as Sulfur Hosts in Lithium Sulfur Batteries. ACS Applied Energy Materials, 2021, 4, 5713-5726.	5.1	11
101	Ultraâ€Large Sized Siloxene Nanosheets as Bifunctional Photocatalyst for a Liâ€O ₂ Battery with Superior Roundâ€Trip Efficiency and Extraâ€Long Durability. Angewandte Chemie, 2021, 133, 11357-11361.	2.0	10
102	Preparation, ion-exchange, and electrochemical behavior of Cs-type manganese oxides with a novel hexagonal-like morphology. Journal of Materials Research, 2007, 22, 2437-2447.	2.6	9
103	Unraveling the Mechanism of the Zn-Improved Catalytic Activity of Pd-Based Catalysts for Water–Gas Shift Reaction. Journal of Physical Chemistry C, 2016, 120, 20181-20191.	3.1	9
104	Design and synthesis of carbon nanofibers decorated by dual-phase TinO2n-1 nanoparticles with synergistic catalytic effect as high performance oxygen reduction reaction catalysts. Electrochimica Acta, 2020, 344, 136120.	5.2	9
105	Cotton fabric-derived hybrid carbon network with N-doped carbon nanotubes grown vertically as flexible multifunctional electrodes for high-rate capacitive energy storage. Journal of Power Sources, 2021, 507, 230303.	7.8	9
106	Sn–Co nanoparticles encapsulated in grid-shell carbon spheres, applied as a high-performance anode material for lithium-ion batteries. RSC Advances, 2015, 5, 53586-53591.	3.6	7
107	Ultrahigh-energy sodium ion capacitors enabled by the enhanced intercalation pseudocapacitance of self-standing Ti2Nb2O9/CNF anodes. Nanoscale, 2021, 13, 15781-15788.	5.6	7
108	Carbon Nanomeshes: Thinâ€6heet Carbon Nanomesh with an Excellent Electrocapacitive Performance (Adv. Funct. Mater. 34/2015). Advanced Functional Materials, 2015, 25, 5406-5406.	14.9	5

#	Article	IF	CITATIONS
109	Reduction degree and property study of graphene nanosheets prepared with different reducing agents and their applicability as a carrier of the Ru(phen) ₃ Cl ₂ luminescent sensor for DNA detection. RSC Advances, 2015, 5, 26856-26862.	3.6	5
110	Atomic Layers: Tellurium-Assisted Epitaxial Growth of Large-Area, Highly Crystalline ReS2 Atomic Layers on Mica Substrate (Adv. Mater. 25/2016). Advanced Materials, 2016, 28, 5018-5018.	21.0	5
111	Phosphate ion functionalized Co3O4 nanosheets/RGO with improved electrochemical performance. Colloids and Surfaces A: Physicochemical and Engineering Aspects, 2020, 586, 124232.	4.7	5
112	On the growth morphology and crystallography of the epitaxial Cu ₇ Te ₄ /CdTe interface. CrystEngComm, 2018, 20, 1050-1056.	2.6	4
113	Lithium Storage in Carbon Cloth–Supported KNb ₃ O ₈ Nanorods Toward a Highâ€Performance Lithiumâ€Ion Capacitor. Small Structures, 2021, 2, 2170021.	12.0	3
114	Few-layer Mg-deficient borophene nanosheets: I ₂ oxidation and ultrasonic delamination from MgB ₂ . Nanoscale, 2022, 14, 4195-4203.	5.6	3
115	Crystal structure of pyridinium tetrahydroxyhexaoxopentaborate pyridine hemisolvate, (C5H6N)[B5O6(OH)4] · ¹⁄2C5H5N. Zeitschrift Fur Kristallographie - New Crystal Structures, 2006, 221, 189-190.	0.3	1
116	New Rare Earth(III) Complexes with H2tmtaa. Chinese Journal of Chemistry, 2006, 24, 1363-1367.	4.9	1
117	Electrochemical Property of Manganese Oxide Nanobelt Bundles with Layered Structure. Chinese Journal of Chemistry, 2012, 30, 299-302.	4.9	1
118	Crystal structure of dimethylammonium bis(salicylato)borate, [NH2(CH3)2][BO4(C7H4O)2]. Zeitschrift Fur Kristallographie - New Crystal Structures, 2006, 221, 179-180.	0.3	0
119	Facile preparation of partially reduced graphite oxide nanosheets as a binder-free electrode for supercapacitors. RSC Advances, 2018, 8, 28987-28996.	3.6	0
120	Research on Fabrication Conditions of TiO2 Pillared Porous Manganese Oxide Nanocompound. Journal of Ion Exchange, 2007, 18, 346-351.	0.3	0